

Color octet contribution to high p_T J/ψ production in pp collisions at $\sqrt{s}=500$ and 200 GeV at BNL RHIC

Gouranga C. Nayak

T-8, Theoretical Division, Los Alamos National Laboratory, Los Alamos, New Mexico 87545, USA

Ming X. Liu

P-25, Physics Division, Los Alamos National Laboratory, Los Alamos, New Mexico 87545, USA

Fred Cooper

T-8, Theoretical Division, Los Alamos National Laboratory, Los Alamos, New Mexico 87545, USA

(Received 3 March 2003; published 7 August 2003)

We compute $d\sigma/dp_T$ of the J/ψ production in pp collisions at BNL RHIC at $\sqrt{s}=500$ and 200 GeV by using both the color octet and singlet models in the framework of nonrelativistic QCD. The J/ψ we compute here includes the direct J/ψ from the partonic fusion processes and the J/ψ coming from the radiative decays of $\chi_{J,S}$ both in the color octet and singlet channel. The high p_T J/ψ production cross section is computed within the PHENIX detector acceptance ranges: $-0.35 < \eta < 0.35$ and $1.2 < |\eta| < 2.4$, the central electron and forward muon arms. It is found that the color octet contribution to J/ψ production is dominant at the BNL Relativistic Heavy Ion Collisions (RHIC) energy in comparison to the color singlet contributions. We compare our results with the recent preliminary data obtained by the PHENIX detector for the high p_T J/ψ measurements. While the color singlet model fails to explain the data completely the color octet model is in agreement with the single data point above 2 GeV transverse momentum. A measurement of J/ψ production at RHIC in the next run with better statistics will allow us to determine the validity of the color octet model of J/ψ production at RHIC energies. This is very important because it is necessary to know the exact mechanism for J/ψ production in pp collisions at RHIC if one is to make predictions of J/ψ suppression as a signature of quark-gluon plasma. These mechanisms also play an important role in determining the polarized spin structure function of the proton at RHIC.

DOI: 10.1103/PhysRevD.68.034003

PACS number(s): 14.40.Gx, 13.85.Hd, 13.85.Ni, 13.87.Fh

Recently there has been much progress in understanding of the heavy quarkonium production mechanism in high energy hadronic collisions. The two prominent models for the heavy quarkonium production mechanism which are quite successful at different collider energies are (1) the color singlet model [1] and (2) the color octet model [2–5]. The J/ψ production measurement by the Collider Detector at Fermilab (CDF) collaboration at Tevatron [6] has ruled out the color singlet model for high p_T quarkonium production [7] in that center of mass energy regime. The color singlet model gives a reasonable description of large p_T J/ψ production at CERN Intersecting Storage Rings (ISR) energies [8]. In this context large p_T J/ψ production data from pp collisions at $\sqrt{s}=500$ and 200 GeV at the BNL Relativistic Heavy Ion Collisions (RHIC) might tell us the relative importance and validity of these two models in this new energy range. In particular a valid J/ψ production mechanism at pp collisions will play an important role in determining the mechanism for J/ψ suppression at Au–Au collisions which is suggested to be a prominent signature for quark-gluon plasma detection at RHIC [9,10]. These mechanisms also play an important role in determining the polarized spin structure function of the proton.

In the color singlet model the quarkonium is formed as a nonrelativistic bound state of heavy quark-antiquark pair via static gluon exchange. In this model it is assumed that the $Q\bar{Q}$ is produced in the color singlet state at the production

point with appropriate spin (S) and orbital angular momentum quantum number (L) to evolve to a bound state $^{2S+1}L_J$ with total angular momentum quantum number (J). The relative momentum of the $Q\bar{Q}$ pair inside the quarkonium is assumed to be small compared to the mass M_Q of the heavy quark so that the Q and \bar{Q} will not fly apart to form heavy mesons. The nonrelativistic nonperturbative wave functions and its derivatives appearing in the color singlet model calculation are either determined from the potential model or taken from experiment.

On the other hand in the color octet model relativistic effects are taken into account which are neglected in the color singlet model. In the color octet model using an effective field theory called nonrelativistic QCD (NRQCD), the dynamical gluon enters into Fock state decompositions of the quarkonium states. In NRQCD the expansion is carried out in terms of the relative velocity v ($v^2 \sim 0.23$ for the $C\bar{C}$ system and 0.1 for the $B\bar{B}$ system) of the $Q\bar{Q}$ bound state. The NRQCD Lagrangian density is given by

$$\mathcal{L}_{\text{NRQCD}} = \mathcal{L}_{\text{light}} + \mathcal{L}_{\text{heavy}} + \mathcal{L}_{\text{correction}}, \quad (1)$$

where

$$\mathcal{L}_{\text{light}} = -\frac{1}{4} F^{a\mu\nu} F_{\mu\nu}^a + \sum \bar{q} \gamma_\mu D^\mu [A] q \quad (2)$$

is the usual QCD Lagrangian for gluons and the light flavors and

$$\mathcal{L}_{\text{heavy}} = \psi^\dagger \left(iD_t + \frac{D^2}{2M} \right) \psi + \phi^\dagger \left(iD_t + \frac{D^2}{2M} \right) \phi \quad (3)$$

is the leading order heavy quark part and

$$\begin{aligned} \mathcal{L}_{\text{correction}} = & \frac{1}{8M^3} [\psi^\dagger D^4 \psi - \phi^\dagger D^4 \phi] \\ & + \frac{g}{8M^2} [\psi^\dagger (D \cdot E - E \cdot D) \psi + \phi^\dagger (D \cdot E - E \cdot D) \phi] \\ & + \frac{ig}{8M^2} [\psi^\dagger \sigma \cdot (D \times E - E \times D) \psi \\ & + \phi^\dagger \sigma \cdot (D \times E - E \times D) \phi] \\ & + \frac{g}{2M} [\psi^\dagger \sigma \cdot B \psi - \phi^\dagger \sigma \cdot B \phi] + \dots \end{aligned} \quad (4)$$

is the correction term. In the above equations ψ, ϕ are the two component Dirac spinors of the heavy quark. The various correction terms in the above equation come from the corrections to kinetic energy, electric field coupling, magnetic field coupling, and from double electric scattering, etc. In NRQCD the dynamical gluon enters into the Fock state decompositions of different physical states. The wave functions of the S -wave orthoquarkonia state $|\psi_Q\rangle$ appear as

$$\begin{aligned} |\psi_Q\rangle = & O(1) |Q\bar{Q}[^3S_1^{(1)}]\rangle + O(v) |Q\bar{Q}[^3P_J^{(8)}]g\rangle \\ & + O(v^2) |Q\bar{Q}[^3S_1^{(1,8)}]gg\rangle + O(v^2) |Q\bar{Q}[^1S_0^{(8)}]g\rangle \\ & + O(v^2) |Q\bar{Q}[^3D_J^{(1,8)}]gg\rangle + \dots \end{aligned} \quad (5)$$

and the wave functions of the P -wave orthoquarkonium state $|\chi_{QJ}\rangle$ appear as

$$|\chi_{QJ}\rangle = O(1) |Q\bar{Q}[^3P_J^{(1)}]\rangle + O(v) |Q\bar{Q}[^3S_1^{(8)}]g\rangle + \dots \quad (6)$$

In the above equation (1),(8) refers to the singlet and octet state of the $Q\bar{Q}$ pair. After a $Q\bar{Q}$ is formed in its color octet state it may absorb a soft gluon and transform into $|\chi_{QJ}\rangle$ via Eq. (6) and then become J/ψ by photon decay or the $Q\bar{Q}$ in the color octet state can emit two long wavelength gluons and become a J/ψ via Eq. (5) and so on. All these low energy interactions are negligible and the nonperturbative matrix elements can be fitted from the experiments or can be determined from the lattice calculations.

Using both mechanisms for heavy quarkonium production we compute the p_T distribution of J/ψ production at RHIC energy in this paper. The J/ψ production includes both direct J/ψ and the J/ψ coming from the radiative decay of χ_J 's: $\chi_J \rightarrow J/\psi + \gamma$. We will calculate the J/ψ production in this paper by considering all the parton fusion processes. In

the color octet model the nonperturbative matrix elements in the parton fusion processes are extracted in [4] by fitting CDF experimental data.

The PHENIX detector at RHIC has measured a few data points in the p_T distribution of J/ψ production at $\sqrt{s} = 200$ GeV pp collisions. As these data are preliminary our comparison to this experimental data is not very conclusive. However, in the future the PHENIX detector at RHIC will measure high p_T J/ψ production up to $p_T \sim 10$ GeV with better statistics. The acceptance range of a single electron for the PHENIX detector is $-0.35 < \eta < 0.35$ and for a single muon it is $1.2 < |\eta| < 2.4$. We compute the transverse momentum distribution of J/ψ production by using both the color octet and the singlet model in the PHENIX detector acceptance range.

The $2 \rightarrow 2$ parton fusion processes which contribute to the p_T distribution of the J/ψ and χ_{cJ} production are of the order of α_s^3 . The differential cross section for the production of a quarkonium state ($^{2S+1}L_J$) with different quantum numbers (L, S, J) in the color singlet model is given by [1]

$$\begin{aligned} & E \frac{d^3\sigma}{d^3p} (AB \rightarrow ^{2S+1}L_J + X) \\ & = \sum_{i,j} \int dx_i x_i f_{i/A}(x_i, Q^2) \int dx_j x_j f_{j/B}(x_j, Q^2) \\ & \quad \times \frac{\hat{s}}{\pi} \frac{d\hat{\sigma}}{d\hat{t}} [ij \rightarrow (^{2S+1}L_J)k] \delta(\hat{s} + \hat{t} + \hat{u} - M^2). \end{aligned} \quad (7)$$

Here x_i and x_j are the momentum fractions carried by partons i and j inside the hadrons A and B , respectively. The $f_{i/A}(x_i)$ and $f_{j/B}(x_j)$ are the parton distribution functions inside the hadron. $d\hat{\sigma}/d\hat{t} [ij \rightarrow (^{2S+1}L_J)k]$ is the partonic level differential cross section to form a quarkonium state ($^{2S+1}L_J$) which involves the radial wave function and its derivatives at the origin. Using the delta function integration in Eq. (7) one obtains

$$\begin{aligned} & \frac{d\sigma}{dp_T} (AB \rightarrow J/\psi, \chi_J + X) \\ & = \sum_{i,j} \int dy \int dx_i x_i f_{i/A}(x_i, Q^2) x_j' f_{j/B}(x_j', Q^2) \\ & \quad \times \frac{2p_T}{M_T} \frac{d\hat{\sigma}}{d\hat{t}} (ij \rightarrow ^{2S+1}L_J k), \end{aligned} \quad (8)$$

where

$$x_j' = \frac{1}{\sqrt{s}} \frac{x_j \sqrt{s} M_T e^{-y} - M^2}{x_j \sqrt{s} - M_T e^y}. \quad (9)$$

In the above M is the mass of the bound state quarkonium and $M_T^2 = \sqrt{p_T^2 + M^2}$. The partonic level differential cross section $d\hat{\sigma}/d\hat{t}[ij \rightarrow ({}^{2S+1}L_J)k]$ for the gluon fusion processes are obtained in [11] by using the helicity decomposition method and the quark, gluon processes are derived in [1]. The $d\hat{\sigma}/d\hat{t}[ij \rightarrow ({}^{2S+1}L_J)k]$ as given in [1] and [11] contain the nonrelativistic wave function $|R(0)|^2$ (for direct J/ψ process) and its derivatives $|R'(0)|^2$ (for χ_J processes) at the origin. For the nonrelativistic wave functions at the origin we take the Buchmuller-type wave function with charm quark mass $M_c = 1.48$ GeV. The numerical value is $|R(0)|^2 = 0.81$ GeV³ [12]. For the derivative of the radial wave function at origin we use $(9/2\pi)|R'(0)|^2/M_c^4 = 15$ MeV [13].

In the color octet model the differential cross section for heavy quarkonium production at order α_s^3 is given by

$$\begin{aligned} & \frac{d\sigma}{dp_T}[AB \rightarrow \psi_Q(\chi_J) + X] \\ &= \sum_{i,j} \int dy \int dx_i x_i f_{i/A}(x_i, Q^2) x_j' f_{j/B}(x_j', Q^2) \\ & \times \times \frac{2p_T}{M_T} \frac{d\hat{\sigma}}{d\hat{t}}(ij \rightarrow C\bar{C}[{}^{2S+1}L_J^{(8)}]k \rightarrow \psi_Q(\chi_J)), \\ & \quad x_i - \frac{e^y}{\sqrt{s}} \end{aligned} \quad (10)$$

where

$$\begin{aligned} & \frac{d\hat{\sigma}}{d\hat{t}}(ij \rightarrow C\bar{C}[{}^{2S+1}L_J^{(8)}]k \rightarrow \psi_Q(\chi_J)) \\ &= \frac{1}{16\pi\hat{s}^2} \sum |\mathcal{A}(ij \rightarrow C\bar{C}[{}^{2S+1}L_J^{(8)}]k)_{\text{short}}|^2 \\ & \times \langle 0 | \mathcal{O}_8^{\psi_Q(\chi_J)}({}^{2S+1}L_J) | 0 \rangle. \end{aligned} \quad (11)$$

In this paper we include the contribution from the ${}^3P_J^{(8)}$ and ${}^1S_0^{(8)}$ processes which are present in the Fock state decomposition amplitude (5) in addition to the ${}^3S_1^{(8)}$ state of the color octet amplitude. A similar process is followed for the χ_J production by using Eq. (6) which takes into account the color octet ${}^3S_1^{(8)}$ state. These χ_J formed in the color octet state again decay radiatively to give J/ψ . The total contribution to J/ψ production in the color octet model is the sum of the direct J/ψ and the contribution coming from χ_J 's decay in the color octet model. In the above equation the short distance part of the partonic matrix element square in different quantum states for various partonic processes, $\sum |\mathcal{A}(ij \rightarrow C\bar{C}[{}^{2S+1}L_J^{(8)}]k)_{\text{short}}|^2$, are very lengthy and are given in [4]. We use all the partonic processes in our calculation. We use the nonperturbative matrix elements, $\langle 0 | \mathcal{O}_8^{\psi_Q(\chi_J)}({}^{2S+1}L_J) | 0 \rangle$, from the tabulation given in [4] which are extracted from the CDF data. In the extraction of

Direct J/ψ Production at RHIC

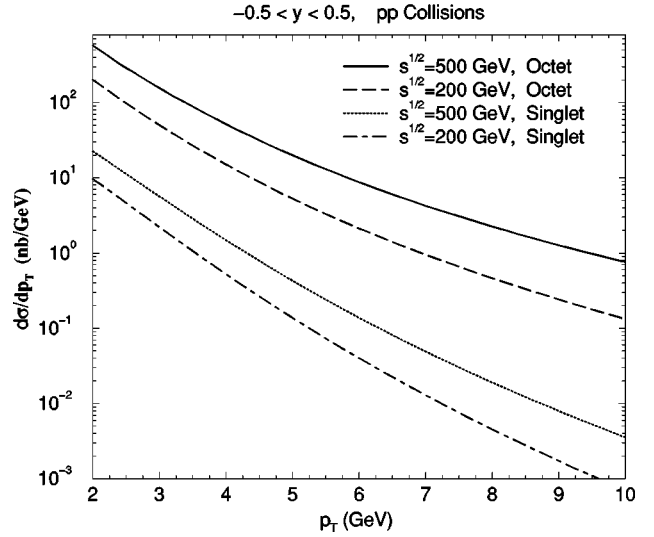


FIG. 1. Direct J/ψ production at RHIC in the J/ψ rapidity range $-0.5 < y < 0.5$.

these matrix elements $\langle 0 | \mathcal{O}_8^{\psi_Q}({}^3P_0) | 0 \rangle = M_Q^2 \langle 0 | \mathcal{O}_8^{\psi_Q}({}^1S_0) | 0 \rangle$ was set and then the values of the linear combination were extracted which is given by $\langle 0 | \mathcal{O}_8^{J/\psi}({}^3P_0) | 0 \rangle / M_c^2 + \langle 0 | \mathcal{O}_8^{J/\psi}({}^1S_0) | 0 \rangle / 3 = (2.2 \pm 0.5) \times 10^{-2}$ GeV³. For other matrix elements the values are given by $\langle 0 | \mathcal{O}_8^{J/\psi}({}^3S_1) | 0 \rangle = (6.6 \pm 2.1) 10^{-3}$ GeV³, $\langle 0 | \mathcal{O}_8^{\chi_1}({}^3S_1) | 0 \rangle = (9.8 \pm 1.3) 10^{-3}$ GeV³. We use the central values of these matrix elements in our calculation.

We present our results for the rapidity range covered by the central electron arm and forward muon arm at the PHENIX detector at RHIC. The electron pseudo rapidity range: $-0.35 < \eta < 0.35$ corresponds to the J/ψ rapidity range: $-0.5 < y < 0.5$. For the muon pseudo rapidity range: $1.2 < |\eta| < 2.4$ we present our results in the J/ψ rapidity range $1 < y < 2$ which is well covered by the RHIC/PHENIX experiment. So the results we will present in this paper are in the J/ψ rapidity range: $-0.5 < y < 0.5$ and $1 < y < 2$. We will use GRV98 NLO [14] parton distribution function throughout our calculation. The Q scale in the structure function and the renormalization scale are chosen to be $Q = M_T = \sqrt{M^2 + p_T^2}$, where M and p_T are the mass and the transverse momentum of the heavy quarkonium, respectively. In extracting the NRQCD matrix elements, the MRSD0 parton distribution functions inside a nucleon was used in the color octet model calculation in [4]. In this paper we are using instead the GRV98 NLO parton distribution function for the parton distribution functions. We have checked that there is no significant difference in the results obtained by using MRSD0 and GRV98 in the quantities calculated here.

In Fig. 1 we present the direct J/ψ production cross section both from the color singlet and color octet models at $\sqrt{s} = 500$ and 200 GeV pp collisions in the J/ψ rapidity range $-0.5 < y < 0.5$. The solid line is the color octet contribution and the dotted line is the color singlet contribution at $\sqrt{s} = 500$ GeV. The dashed line is the color octet contribution

J/ψ from χ_{cJ} Decays at RHIC

$-0.5 < y < 0.5$, pp Collisions

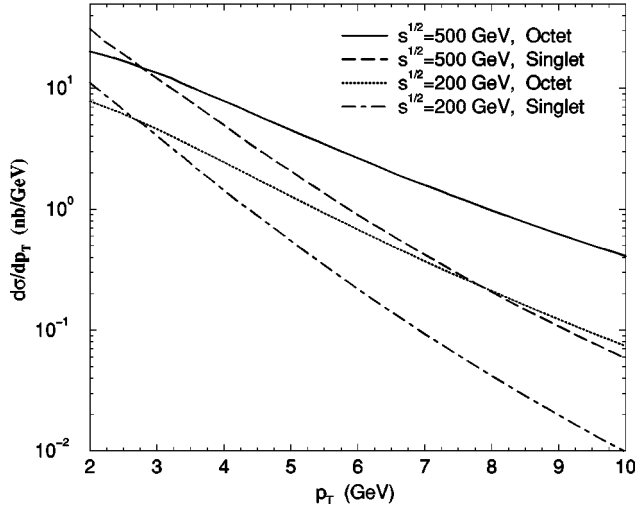


FIG. 2. J/ψ production cross section at RHIC from the χ_{cJ} 's decay in the J/ψ rapidity range $-0.5 < y < 0.5$.

and the dot-dashed line is the color singlet contribution at $\sqrt{s} = 200$ GeV. The direct J/ψ production from the color octet model at both the colliding energies is much higher than the color singlet counterparts. In what follows, we present the results of our computation for the p_T range from 2 to 10 GeV. At smaller p_T , the color singlet and octet cross sections are corrupted by collinear divergences as discussed in [3,4]. Since the intrinsic motion of the incident partons inside colliding protons renders the differential cross section uncertain for $p_T \leq 2$ GeV, as discussed in [3,4] we have presented our results for $p_T \geq 2$ GeV in this paper. For low p_T calculation one might follow the procedure where one might have to take intrinsic motion of the incident parton into account. This calculation is, however, beyond the scope of the present paper. In this paper we report the predictions for high p_T J/ψ production. A high p_T limit of ~ 10 GeV corresponds to the possible p_T measurement range at PHENIX. In the very high p_T limit (≥ 6 GeV) the B decay contribution $B \rightarrow J/\psi + X$ and the gluon and charm quark fragmentation contribution might become important. However, we have not included these processes here. In this paper we have computed only the prompt J/ψ production from the parton fusion processes. These are the same contributions that were used in [4] at Tevatron energies to extract NRQCD matrix elements.

In Fig. 2 we present the predictions for the J/ψ production cross section coming from the radiative decay of the χ_{cJ} 's both from the color octet and singlet model at $\sqrt{s} = 500$ and 200 GeV pp collisions in the J/ψ rapidity range $-0.5 < y < 0.5$. The solid line is the color octet contribution and the dashed line is the color singlet contribution at $\sqrt{s} = 500$ GeV. The dotted line is the color octet contribution and the dot-dashed line is the color singlet contribution at $\sqrt{s} = 200$ GeV. The χ_{cJ} contribution in each case in the figure is the sum of the contributions from χ_0 , χ_1 , and χ_2 . The χ_{cJ} 's decay coming from the color singlet channel is slightly higher at small p_T but very much lower at large p_T in com-

Direct J/ψ Production at RHIC

$1 < y < 2$, pp Collisions

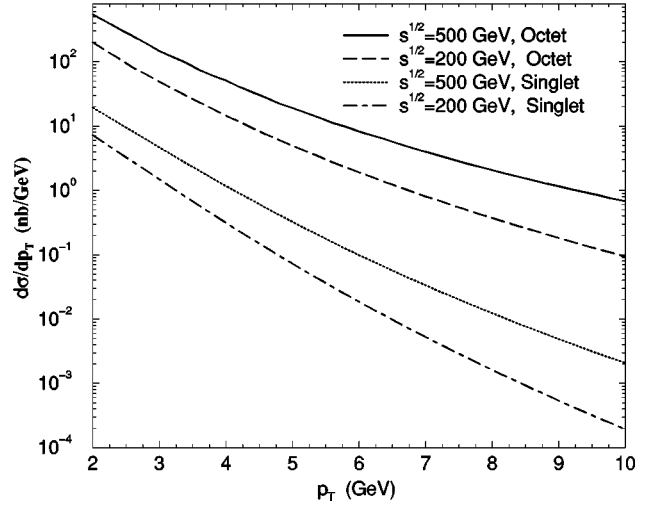


FIG. 3. Direct J/ψ production at RHIC in the J/ψ rapidity range $1 < y < 2$.

parison to the color octet contribution. It can also be noted from Figs. 1 and 2 that the direct J/ψ production in the color octet channel is larger than the contributions coming from all other processes. Thus at RHIC energies, we find that the dominant contribution to J/ψ production comes from this direct color octet process.

In Fig. 3 we present the results of our computation for the direct J/ψ production for both the color singlet and octet models in the J/ψ rapidity range $1 < y < 2$ at $\sqrt{s} = 500$ and 200 GeV. The solid line is the contribution from the color octet process and the dotted line is the contribution from the color singlet process at $\sqrt{s} = 500$ GeV. The dashed line and dot-dashed lines are the similar curves at $\sqrt{s} = 200$ GeV. In this rapidity regime we also find that the color octet contribution is much larger than the color singlet contribution. In Fig. 4 we present the J/ψ production cross section coming from the χ_{cJ} 's decay in the J/ψ rapidity range $1 < y < 2$ at $\sqrt{s} = 500$ and 200 GeV pp collisions at RHIC. The solid line is the contribution from the color octet process and the dashed line is the contribution from the color singlet process at $\sqrt{s} = 500$ GeV. The dotted line and dot-dashed lines are the similar curves at $\sqrt{s} = 200$ GeV. The total χ_{cJ} contributions in the figure includes the contributions from χ_0 , χ_1 , and χ_2 . As ψ' contribution to J/ψ is small at this energy range we have not considered the ψ' contribution in our calculation. As can be seen again the dominant contribution to the J/ψ production comes mainly from the direct J/ψ production in the color octet channel.

The total $J/\psi p_T$ distribution coming from the combined color singlet model and color octet model contributions in all channels is plotted in Fig. 5 in the J/ψ rapidity range $-0.5 < y < 0.5$ at $\sqrt{s} = 500$ and 200 GeV pp collisions. The solid line is the p_T distribution of the total [octet (direct $J/\psi + \chi_{cJ}$'s decay) plus singlet (direct $J/\psi + \chi_{cJ}$'s decay)] J/ψ production cross section at $\sqrt{s} = 500$ GeV. The dashed line is the contribution from the color octet model and the dot-

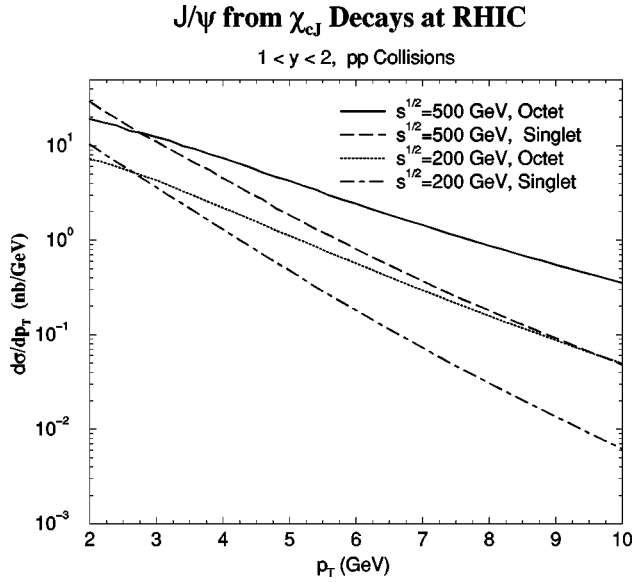


FIG. 4. J/ψ production cross section at RHIC from the χ_{cJ} 's decay in the J/ψ rapidity range $1 < y < 2$.

dashed line is the contribution from the singlet model at the same energy. As pointed out in the above the total cross section is the sum of the cross section from direct J/ψ and from the radiative decays of the χ_J 's both in color octet and singlet channels. It can be seen that the total cross section is almost the same as the cross section obtained from the color octet channels. The color singlet channel contribution is very small as can be seen from the dot-dashed line.

Similar results are obtained for $\sqrt{s}=200$ GeV pp collisions in the same figure in the J/ψ rapidity range $-0.5 < y < 0.5$. The dotted line is the total [octet (direct $J/\psi + \chi_J$'s decay) plus singlet (direct $J/\psi + \chi_J$'s decay)] J/ψ production cross section at $\sqrt{s}=200$ GeV. A long-dashed line is the octet contribution and a thin-solid line is the singlet contribu-

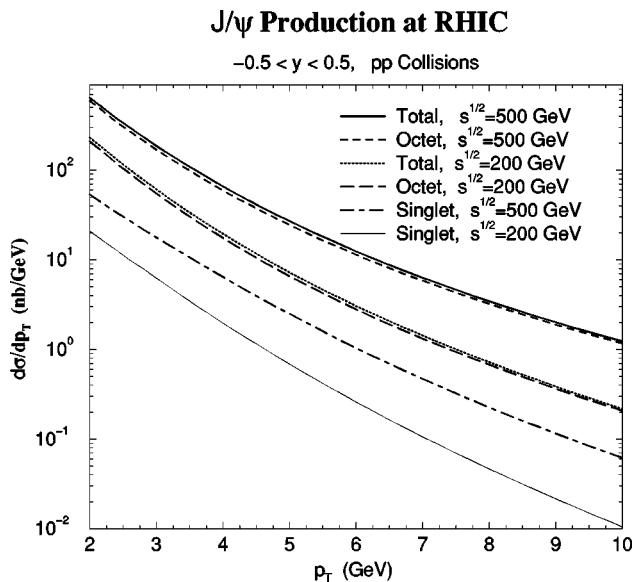


FIG. 5. J/ψ production at RHIC from parton fusion processes in the J/ψ rapidity range $-0.5 < y < 0.5$.

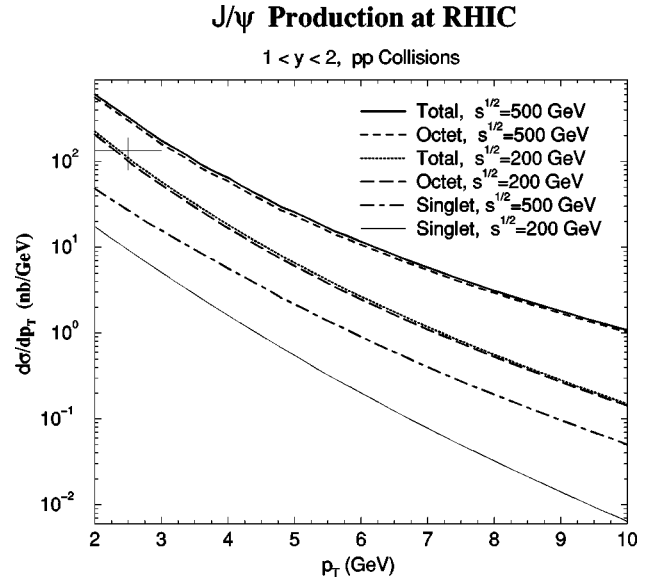


FIG. 6. J/ψ production at RHIC from the parton fusion processes in the J/ψ rapidity range $1 < y < 2$.

tion. It can be seen from the figure that the total J/ψ production cross section is almost the same as that of the color octet model contribution and the singlet contribution is much smaller. A measurement of the J/ψ differential cross section at RHIC in the future (both at $\sqrt{s}=500$ and 200 GeV pp collisions) will be able to tell us whether the color octet model reproduces the RHIC data.

As PHENIX has measured few data points for p_T distribution of J/ψ in the $\mu^+ \mu^-$ rapidity range in pp collisions at $\sqrt{s}=200$ GeV, we will compare our results with the available experimental data. As stated earlier we will compare the available data in the J/ψ rapidity range $1 < y < 2$ as this range is well covered by the RHIC/PHENIX experiment in the muon channel. In Fig. 6 we present the p_T distribution of the total J/ψ production cross section from the color singlet and octet model in the J/ψ rapidity range $1 < y < 2$ at $\sqrt{s}=500$ GeV. The solid line is the p_T distribution of the total [octet (direct $J/\psi + \chi_J$'s decay) plus singlet (direct $J/\psi + \chi_J$'s decay)] J/ψ production cross section at $\sqrt{s}=500$ GeV. The dashed line is the contribution from the color octet model and the dot-dashed line is the contribution from the singlet model at the same energy. The p_T distribution of the total J/ψ production cross section from the color octet and singlet model in the J/ψ rapidity range $1 < y < 2$ at $\sqrt{s}=200$ GeV pp collisions is plotted in Fig. 6. The dotted line is the total [octet (direct $J/\psi + \chi_J$'s decay) plus singlet (direct $J/\psi + \chi_J$'s decay)] J/ψ production cross section at $\sqrt{s}=200$ GeV. The long-dashed line is the octet contribution and the thin-solid line is the singlet contribution.

Let us compare our results with the preliminary experimental data obtained at the PHENIX detector. As mentioned earlier, at small p_T the color singlet and octet cross sections are corrupted by collinear divergences as discussed in [4]. Since the intrinsic motion of the incident partons inside colliding protons renders the differential cross section uncertain for $p_T \leq 2$ GeV, as discussed in [3,4] we will compare our

results at $p_T \geq 2$ GeV with the PHENIX data [15] in this paper. We compare our calculation with the only available data point (≥ 2 GeV) at $p_T \sim 2.5$ GeV (see [15]). The data point is presented as “+” in Fig. 6. It can be seen that the present experimental data fits the color octet model predictions of J/ψ production and the color singlet model prediction is well below the data point. Hence the color singlet model is not the relevant mechanism at RHIC energy. As for the color octet model, the single data point matches with the color octet contribution, but many more data with high precision measurements are necessary to confirm the validity of the color octet model at RHIC energy. The next run results from the PHENIX experiment will be able to shed light on this.

In summary, we have computed the J/ψ production differential cross section in pp collisions at RHIC at $\sqrt{s} = 500$ and 200 GeV by using both the color octet and singlet models in the framework of nonrelativistic QCD. The J/ψ production cross section we compute here includes the direct J/ψ production from the partonic fusion processes and the J/ψ coming from the radiative decays of χ_J 's both in the color octet and singlet channel. The high p_T J/ψ production cross section is computed within the J/ψ rapidity range,

$-0.5 < y < 0.5$ and $1 < |\eta| < 2$, in the central electron and forward muon arms, respectively. It is found that the color octet contribution to J/ψ production is dominant at RHIC energy in comparison to the color singlet contributions. We have compared our results with the recent data obtained by the PHENIX detector for $p_T \geq 2$ GeV at $\sqrt{s} = 200$ GeV pp collisions. While the color singlet model fails to explain the data completely the color octet model seems to reproduce the data. As the present high p_T data of J/ψ production at the PHENIX detector at RHIC is very restricted, measurement of high $p_T J/\psi$ production at the RHIC in the next run with better statistics will be able to tell us the degree of validity of the color octet model of J/ψ production at RHIC energies. It is necessary to know the exact mechanism of J/ψ production in pp collisions at RHIC in order to make a prediction of J/ψ suppression as a signature of the quark-gluon plasma in Au–Au collisions. Knowledge of the J/ψ production mechanism is also crucial for isolating the polarized spin structure functions of the proton from the data.

This research was supported by the Department of Energy, under contract W-7405-ENG-36. We thank Rajiv Gavai, Mike Leitch, Pat McGaughey, Emil Mottola, and Johann Rafelski for useful discussions.

-
- [1] E. L. Berger and D. Jones, Phys. Rev. D **23**, 1521 (1981); R. Baier and R. Ruckl, Z. Phys. C **19**, 251 (1983).
- [2] G. T. Bodwin, E. Braaten, and G. P. Lepage, Phys. Rev. D **51**, 1125 (1995); **55**, 5853 (1997).
- [3] P. Cho and A. K. Leibovich, Phys. Rev. D **53**, 150 (1996).
- [4] P. Cho and A. K. Leibovich, Phys. Rev. D **53**, 6203 (1996).
- [5] E. Braaten, M. A. Doncheski, S. Fleming, and M. Mangano, Phys. Lett. B **333**, 548 (1994); D. P. Roy and K. Sridhar, *ibid.* **339**, 141 (1994); M. Cacciari and M. Greco, Phys. Rev. Lett. **73**, 1586 (1994); G. T. Bodwin, E. Braaten, and G. P. Lepage, Phys. Rev. D **46**, R1914 (1992); E. Braaten and S. Fleming, Phys. Rev. Lett. **74**, 3327 (1995); S. Gupta and K. Sridhar, Phys. Rev. D **54**, 5545 (1996); **55**, 2650 (1997); M. Cacciari and M. Kramer, Phys. Rev. Lett. **76**, 4128 (1996); M. Beneke and I. Rothstein, Phys. Rev. D **54**, 2005 (1996).
- [6] CDF Collaboration, F. Abe *et al.*, Phys. Rev. Lett. **75**, 4358 (1995); CDF Collaboration, Report No. Fermilab-Conf-94/136-E, 1994; Fermilab-Conf-95/128-E, 1995.
- [7] E. Braaten, S. Fleming, and T. C. Yuan, Annu. Rev. Nucl. Part. Sci. **46**, 197 (1996), and references therein.
- [8] A. G. Clark *et al.*, Nucl. Phys. **B142**, 29 (1978); K. Ueno *et al.*, Phys. Rev. Lett. **42**, 486 (1979); C. Kourkoumelis *et al.*, Phys. Lett. **91B**, 481 (1980).
- [9] T. Matsui and H. Satz, Phys. Lett. B **178**, 416 (1986); X.-M. Xu *et al.*, Phys. Rev. C **53**, 3051 (1996); G. C. Nayak, J. High Energy Phys. **02**, 005 (1998); Phys. Lett. B **442**, 427 (1998).
- [10] F. Cooper, E. Mottola, and G. C. Nayak, Phys. Lett. B **555**, 181 (2003); G. C. Nayak, A. Dumitru, L. McLerran, and W. Greiner, Nucl. Phys. **A687**, 457 (2001), and references therein.
- [11] R. Gastmans, W. Troost, and T. T. Wu, Nucl. Phys. **B291**, 731 (1987).
- [12] E. J. Eichten and C. Quigg, Phys. Rev. D **52**, 1726 (1995).
- [13] G. T. Bodwin, E. Braaten, and G. P. Lepage, Phys. Rev. D **46**, 1914 (1992).
- [14] M. Glück, E. Reya, and A. Vogt, Eur. Phys. J. C **5**, 461 (1998).
- [15] A. D. Frawley, for the PHENIX Collaboration, 16th International Conference on Ultrarelativistic Nucleus-Nucleus Collisions, Quark Matter 2002 (QM2002), Nantes, France, 2002, nucl-ex/0210013; and for p_T distribution data see: <http://www.phenix.bnl.gov/conferences.html>